Monitoring the propagation of mechanical waves using an optical fiber distributed and dynamic strain sensor based on BOTDA

Yair Peled,[1,*] Avi Motil,[1] Iddo Kressel,[2] and Moshe Tur[1]

[1]*The Faculty of Engineering, Tel-Aviv University, Tel-Aviv 69978, Israel*
[2]*Israel Aerospace Industries, Israel*
[*]*yairpeled@gmail.com*

Abstract: We report a Brillouin-based fully distributed and dynamic monitoring of the strain induced by a propagating mechanical wave along a 20m long composite strip, to which surface a single-mode optical fiber was glued. Employing a simplified version of the Slope-Assisted Brillouin Optical Time Domain Analysis (SA-BOTDA) technique, the whole length of the strip was interrogated every 10ms (strip sampling rate of 100Hz) with a spatial resolution of the order of 1m. A dynamic spatially and temporally continuous map of the strain was obtained, whose temporal behavior at four discrete locations was verified against co-located fiber Bragg gratings. With a trade-off among sampling rate, range and signal to noise ratio, kHz sampling rates and hundreds of meters of range can be obtained with resolution down to a few centimeters.

OCIS codes: (060.2370) Fiber optics sensors; (290.5830) Brillouin scattering; (330.1880) Detection; (190.0190) Nonlinear optics.

References and links

1. A. Othonos and K. Kalli, *Fiber Bragg Gratings* (Artech House, 1999).
2. B. A. Childers, M. E. Froggatt, S. G. Allison, T. C. Moore, Sr., D. A. Hare, C. F. Batten, and D. C. Jegley, "Use of 3000 Bragg grating strain sensors distributed on four 8-m optical fibers during static load tests of a composite structure," Proc. SPIE **4332**, 133–142 (2001).
3. M. Froggatt and J. Moore, "High resolution strain measurement in optical fiber with Rayleigh scatter," Appl. Opt. **37**, 1735–1740 (1998).
4. D. P. Zhou, Z. Qin, W. Li, L. Chen, and X. Bao, "Distributed vibration sensing with time-resolved optical frequency-domain reflectometry," Opt. Express **20**(12), 13138–13145 (2012).
5. T. Kurashima, T. Horiguchi, and M. Tateda, "Distributed-temperature sensing using stimulated Brillouin scattering in optical silica fibers," Opt. Lett. **15**(18), 1038–1040 (1990).
6. L. Thévenaz, "Inelastic Scatterings and Applications to Distributed Sensing" in *Advanced Fiber Optics - Concepts and Technology, Thévenaz L.* ed, (Switzerland: EPFL University, 2011).
7. X. Bao and L. Chen, "Recent progress in distributed fiber optic sensors," Sensors (Basel) **12**, 8601–8639 (2012).
8. W. Li, X. Bao, Y. Li, and L. Chen, "Differential pulse-width pair BOTDA for high spatial resolution sensing," Opt. Express **16**(26), 21616–21625 (2008).
9. S. M. Foaleng, M. Tur, J. C. Beugnot, and L. Thevenaz, "High spatial and spectral resolution long-range sensing using Brillouin echoes," J. Lightwave Technol. **28**(20), 2993–3003 (2010).
10. T. Sperber, A. Eyal, M. Tur, and L. Thévenaz, "High spatial resolution distributed sensing in optical fibers by Brillouin gain-profile tracing," Opt. Express **18**(8), 8671–8679 (2010).
11. A. W. Brown, B. G. Colpitts, and K. Brown, "Dark-pulse Brillouin optical time-domain sensor with 20-mm spatial resolution," J. Lightwave Technol. **25**(1), 381–386 (2007).
12. K. Hotate and S. S. L. Ong, "Distributed fiber Brillouin strain sensing by correlation-based continuous-wave technique ~cm-order spatial resolution and dynamic strain measurement," Proc. SPIE **4920**, 299–310 (2002).
13. R. Bernini, A. Minardo, and L. Zeni, "Dynamic strain measurement in optical fibers by stimulated Brillouin scattering," Opt. Lett. **34**(17), 2613–2615 (2009).
14. Y. Peled, A. Motil, L. Yaron, and M. Tur, "Slope-assisted fast distributed sensing in optical fibers with arbitrary Brillouin profile," Opt. Express **19**(21), 19845–19854 (2011).
15. K. Y. Song, M. Kishi, Z. He, and K. Hotate, "High-repetition-rate distributed Brillouin sensor based on optical correlation-domain analysis with differential frequency modulation," Opt. Lett. **36**(11), 2062–2064 (2011).

#184596 - $15.00 USD Received 31 Jan 2013; revised 13 Mar 2013; accepted 17 Mar 2013; published 24 Apr 2013

16. Y. Peled, A. Motil, and M. Tur, "Fast Brillouin optical time domain analysis for dynamic sensing," Opt. Express **20**(8), 8584–8591 (2012).
17. A. Voskoboinik, J. Wang, B. Shamee, S. R. Nuccio, L. Zhang, M. Chitgarha, A. E. Willner, and M. Tur, "SBS-based fiber optical sensing using frequency-domain simultaneous tone interrogation," J. Lightwave Technol. **29**(11), 1729–1735 (2011).
18. T. Yari, K. Nagai, and K. Hotate, "Monitoring aircraft structural health using optical fiber sensors," Mitsubishi Heavy Ind. Tech. Rev. **45**, 5–8 (2008).
19. A. Motil, Y. Peled, L. Yaron, and M. Tur, "BOTDA measurements in the presence of fiber vibrations," Proc. SPIE **8351**, 835132, 835132-6 (2012).
20. J. Urricelqui, A. Zornoza, M. Sagues, and A. Loayssa, "Dynamic BOTDA measurements based on Brillouin phase-shift and RF demodulation," Opt. Express **20**(24), 26942–26949 (2012).
21. J. C. Beugnot, M. Tur, S. F. Mafang, and L. Thévenaz, "Distributed Brillouin sensing with sub-meter spatial resolution: modeling and processing," Opt. Express **19**(8), 7381–7397 (2011).
22. S. Timoshenko and D. N. Young, *Vibration Problems in Engineering* (V. Nostrand, N.J., 1955).

1. Introduction

Fiber-optic sensing has already proven itself as an effective way to monitor strain and temperature in structural health monitoring (SHM), as well as in many security applications from border fences to oil and gas pipes. Recent studies have indicated that many of these applications (e.g., effective damage detection) can benefit from sensing, which is both spatially continuous and dynamic (a few hundred Hertz).

The leading fiber-optic sensing technique today utilizes Fiber Bragg Gratings (FBG) [1]. While FBGs are excellent sensors of both static and dynamic events, they have two main disadvantages: (*i*) They have to be written on the fiber, raising the sensor cost; (*ii*) Most currently available interrogators, relying on non-overlapping spectral reflections from the different FBGs, can handle only a relatively small number of multiplexed sensors on the same fiber, thereby making the sensing spatially discrete. While optical frequency domain reflectometry (OFDR) can handle many more spectrally overlapping FBGs on a single fiber [2], the technique is currently limited in terms of range and speed. Sharing the same limitations are OFDR techniques which use Rayleigh backscattering to provide distributed sensing with the required spatial resolution [3,4]. To achieve both high spatial resolution (~cm's) and fast sensing (100's Hertz) on a standard untreated fiber over practical ranges of 100's of meters, we turn our attention to a sensing technique, based on the nonlinear Brillouin scattering effect.

The Brillouin effect in optical fibers is now widely utilized for strain/temperature monitoring of quite a few structures such as long gas pipes, undersea electrical cables, tunnels and more [5–7]. The most common technique is Brillouin Optical time Domain Analysis (BOTDA) [6], where a pump pulse wave, launched into one end of the sensing fiber, nonlinearly interacts with a counter-propagating CW probe wave launched from the fiber opposite side. By scanning the relative optical frequency between the pump and probe waves, the frequency of maximum interaction can be determined, from which the values of the local strain/temperature are extracted. Spatial resolution has been significantly improved recently, down to centimeters [8–11]. While BOTDA can cover tens of kilometers, the method is very slow (seconds to many minutes). Recently, a few methods were developed to enable Brillouin dynamic sensing [12–18]. One of them is the slope-assisted (SA-BOTDA) [14], which retains all advantages of the classical BOTDA while providing true distributed sensing over hundreds of meters of fiber, having an arbitrary longitudinal Brillouin profile. As in classical BOTDA each pump pulse generates information from the whole length of the fiber. With this technique sampling rates are limited only by the time-of-flight of light in the fiber, reaching 1MHz (100kHz) for a fiber total length of 100m (1km), before averaging. In this paper we apply the SA-BOTDA technique to the measurement of the dynamic strains associated with mechanical flexural waves along a 20m composite strip. Results are compared at a few discrete points with those of co-located fiber Bragg gratings (FBGs).

#184596 - $15.00 USD Received 31 Jan 2013; revised 13 Mar 2013; accepted 17 Mar 2013; published 24 Apr 2013

2. Method

We first measure the Brillouin Gain Spectrum (BGS) along the fiber under test using classical BOTDA. While normally maintaining its shape and width, the BGS position in frequency (with respect to that of the pump) may change along the fiber in response to changing strain and temperature conditions. In the SA-BOTDA technique we refer to the (frequency) center of the linear section of one of the slopes of the BGS of each segment along the fiber (as defined by the achievable spatial resolution) as that segment's 'working point', see Fig. 1. In case the segment is vibrating, we pick the working point from the long-term average measurement of the segment BGS [19]. We then fix the frequency of the probe to that of the working point. Local dynamic strain will shift the local BGS to higher or lower frequencies by ~50MHz/1000με for standard single mode fibers at 1550nm, thereby dynamically changing the local Brillouin gain experienced by the probe, Fig. 1. The temporal gain increases or decreases, with respect to the gain at the working point, depending on the direction of the temporal BGS shift. The useful dynamic range for strain/temperature measurements depends on the frequency extent of the slope, which is of the order of the full-width-half-maximum (FWHM) of the BGS (or of the order of twice that number for slope phase interrogation [20]). In practice, pump pulse widths longer than ~50ns provide a dynamic range of ~600με, which increases for shorter pulse widths [21], at the expense of shallower slopes (i.e., lower frequency-to-strain sensitivity). Due to the normally *non-uniform* distribution of static (or 'averaged') strain and temperature along the fiber, the optimal frequency of the working point is not fixed but rather location-dependent. These longitudinal variations pose no problem, as long as they are well contained within the extent of the linear slope, still leaving room on the slope for dynamic strain variations. Under this condition, the local dynamic strain at each spatial position along the fiber is derived by subtracting the mean gain from the measured one.

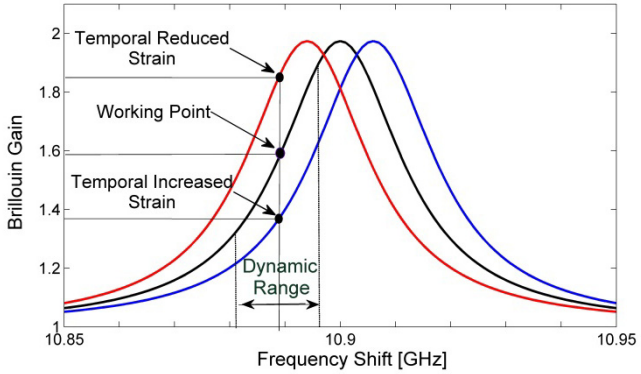

Fig. 1. Brillouin gain spectra of a fiber segment under time average (black), high (blue) and low (red) strain values. A frequency working point is chosen near the center of the left slope; see the black point on the black Lorentzian. Positive (negative) strains introduced to the fiber, shift the BGS to higher (lower) frequencies, thereby modulating the Brillouin gain experienced by the propagating probe wave.

If a larger dynamic range is required (due to larger variations of the static BGS distribution), shorter pump pulses can be used, widening the gain spectrum linewidth and its linear slop range, respectively. The more complex scenario, where the static variations exceed the extent of the slope, can be uncompromisingly handled by tailoring a special probe wave to fit the Brillouin profile of the fiber, as demonstrated in [14].

#184596 - $15.00 USD Received 31 Jan 2013; revised 13 Mar 2013; accepted 17 Mar 2013; published 24 Apr 2013

3. The experimental setup

The focus of this paper is the real-time distributed measurement of mechanical waves propagating along a 20m long, 50mm wide, and 1.4mm thick high-modulus reinforced composite strip. Eighty five meters of a standard single-mode fiber (SMF-28) were used, of which 20m were attached to the upper surface of the strip under mild tension, Fig. 2. With the purpose of verifying that the SA-BOTDA technique correctly measures the dynamic strain along the fiber we added another glued fiber, having four inscribed FBGs with stress free reflection peaks at 1535, 1544, 1550 and 1559nm (our FBGs did not have low enough side-lobes to allow them to be parts of the first fiber without interfering with the Brillouin-based sensing).

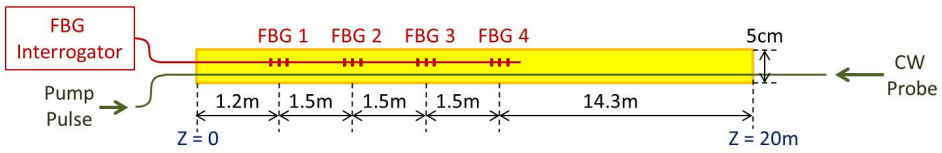

Fig. 2. The composite strip with two glued fibers: the long one for the Brillouin sensing and the short one for measurement validation using fiber Bragg gratings.

The FBGs were measured by a commercial interrogator at a sampling rate of 1kHz. Strain values (ε) were deduced from the well-known relation: $\Delta\lambda(z,t)/\lambda(z) = 0.78\varepsilon(z,t)$ [1], where $\Delta\lambda$ is the strain-induced wavelength deviation from $\lambda(z)$, which is the resting value of the FBG peak reflection wavelength at z.

For the SA-BOTDA method we used the setup of Fig. 3. We first performed a classical BOTDA characterization of the resting strip by sweeping the optical frequency of the CW probe (in 1MHz steps) over the BGS while using 13nsec-wide pump pulses and a fast polarization scrambler. Two hundred and fifty measurements were made per interrogation frequency in order to average over noise and polarization. Figure 4 shows the measured Brillouin Frequency Shift (BFS, red), as well as the two mid-slope contours of the BGS (Fig. 1) along the Sample Under Test (SUT). These measurements indicate a rather uniformly strained fiber with a Brillouin width of ~80MHz, which is commensurate with a 13ns pump pulse width [6]. In the slope-assisted mode of operation of the setup, both pump and probe frequencies were constant and their difference was tuned (by the microwave signal generator) to sit on the middle of that slope of the BGS for which a positive strain gives rise to higher Brillouin gain (Figs. 1 and 4). The SUT was interrogated at an effective (including averaging) rate of 100Hz by bursts of 13ns pump pulses, where each burst contained 250 pulses, launched with a repetition rate of 1MHz (allowing the interrogation of up to 100m long fiber). The intensity of the Brillouin amplified probe was detected by a photo-detector and digitized by a deep memory oscilloscope at a rate of 1GSamples/sec. To save memory, data collection was active only during the duration of the bursts, which occupied only 2.5% of the total time (250μs out of 10ms). Representing different realizations of polarization and noise, the 250 successive SUT interrogations of each burst were averaged to obtain one temporal measurement of the strain distribution along the strip.

Finally, equipped with the previously measured strain sensitivity of the fiber BFS, we dithered the probe frequency around the mid-slope point, while measuring the probe output intensity, thereby achieving the required conversion factor between strain and probe gain.

#184596 - $15.00 USD Received 31 Jan 2013; revised 13 Mar 2013; accepted 17 Mar 2013; published 24 Apr 2013

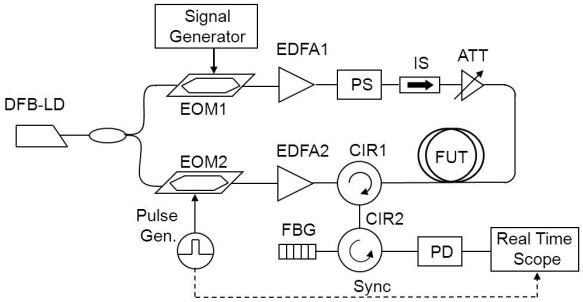

Fig. 3. Experimental setup: DFB-LD: Narrow linewidth (<10kHz) laser diode, EOM: electro-optic modulator, EDFA: Erbium-doped fiber amplifier, CIR: circulator, FBG: fiber Bragg grating, PS: polarization scrambler, IS: isolator, ATT: attenuator, PD: photodiode, FUT: fiber under test.

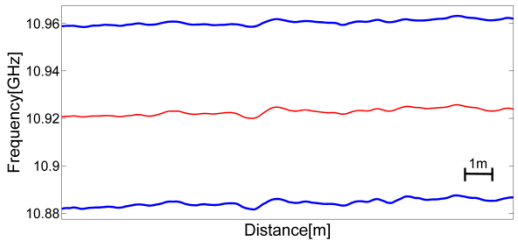

Fig. 4. The BFS (red) along the strip, together with −3dB mid-slope contours, showing quite a small dependence on distance and a BGS linewidth of 80MHz. With such a small distance variation of the −3dB contours, there is no need for a tailored probe wave, as in [14], and a CW probe fixed frequency of 10.96MHz was used.

4. The flexural wave

A flexural bell-shaped mechanical wave was manually excited from the $z = 0$ end of the strip (Fig. 5(a), Media 1), and propagated towards the other end, with an initial peak height of ~0.35m and a spatial width at half peak height of ~2m. Let $y(z,t)$ denote the strip vertical displacement at distance z and time t. Neglecting tensile extension and shear deformation the local strain at the top surface of the strip, where the fiber is glued is given by [22]:

$$\varepsilon = -\frac{w}{2}\frac{\partial^2 y}{\partial z^2}, \tag{1}$$

where w is the strip thickness. For simulation purposes a Gaussian shape of the displacement $y(z,t)$ was used to model the mechanical wave with parameters (height and width) chosen to approximate those of the experiment. Its shape, together with the associated expected strain, $\varepsilon(z,t)$, appear in Fig. 5(b).

#184596 - $15.00 USD Received 31 Jan 2013; revised 13 Mar 2013; accepted 17 Mar 2013; published 24 Apr 2013

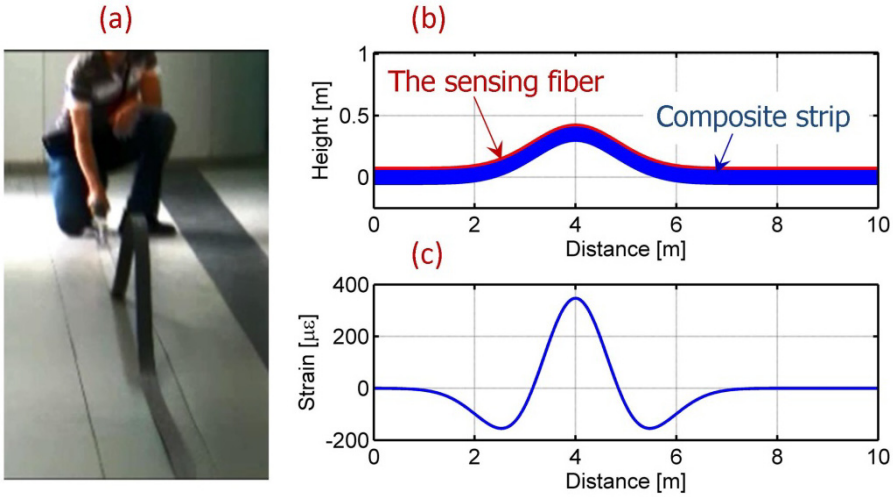

Fig. 5. (a) A single-frame from the recorded movie (Media 1) showing the flexural bell-shaped wave. (b) A Gaussian-modeled flexural wave along the strip (blue). The sensing fiber (red) is glued to the strip top surface. (c) The corresponding strain wave at the strip top surface. While the real wave is not Gaussian, the model wave height (0.35m), as well as its FWHM spatial width (2m), were chosen to produce a strain wave having spatial scales similar to those observed in the experiment.

Note that the modeled spatial distribution of the strain is characterized by scales on the order of 1meter. Such scales will be easily resolved by ~1cm long FBGs. As for Brillouin sensing in basic BOTDA configurations, excluding those employing resolution enhancement techniques [8–11] it is generally assumed that the spatial resolution is of the order of the pump pulse width. At 13ns this pulse width translates into 1.3m, which seems to be a bit too short to resolve the expected details. Therefore, a careful analysis of the current scenario was performed using a perturbation solution of the relevant electromagnetic and acoustic wave equations, described in detail in [9,21] and modified to simulate the SA-BOTDA configuration. The analysis takes full account of all physical phenomena involved, including the finite phonon lifetime (6ns). Its only limitation is the assumption of weak Brillouin gain. With an observed velocity of the flexural wave of the order of 10m/s, we could safely assume a static scenario, where the Gaussian spatial distribution of the strain, centered, *e.g.*, at 4m from the beginning of the strip, induces a corresponding spatial distribution of the BFS, using a conversion factor of 50MHz/1000με.

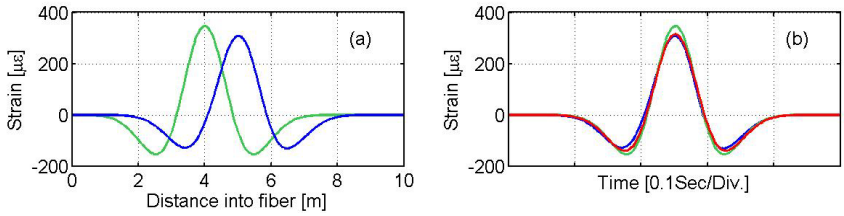

Fig. 6. Theoretical predictions for the expected Brillouin-determined induced strain along the strip. (a) The modeled strain (green) and the Brillouin result (blue). Note the only slight reductions in the positive and negative peaks and also the delayed response. (b) Time aligned temporal signatures of the strain (assuming a velocity of 10m/s for the flexural wave): The Brillouin results (blue), strain readings from a *short* FBG (green) and temporally smoothed FBG results (red).

A square 13ns-wide pump pulse was launched into the fiber at the strip left hand side, see Fig. 2. Strain information at distance z along the fiber was extracted from the time

#184596 - $15.00 USD Received 31 Jan 2013; revised 13 Mar 2013; accepted 17 Mar 2013; published 24 Apr 2013

dependence of the probe power at the strip entrance using the conversion relation $z = V_g t / 2$, where V_g is the light group velocity and $t = 0$ is when the leading edge of pump pulse enters the strip. Figure 6(a) shows the spatial form of the Brillouin results (blue), together with the corresponding shape of the input strain (green). Clearly, the 13ns pump pulse only slightly reduces the positive and negative peaks of the strain wave, while preserving its overall shape. Note, however, that the Brillouin predicted spatial distribution of the strain appears to be delayed with respect to the true strain. Originating from the *gradual* buildup of the acoustic field in response to a *square* pump pulse [21], this delay is a function of: (*i*) The phonon lifetime; (*ii*) The pump pulse width; and (*iii*) The choice of the time origin in the conversion of the Brillouin temporal signal into distance along the strip (choosing the trailing edge of the pump pulse as the time origin results in a negative delay). The nature of this function and signal processing techniques to alleviate this delay issue are under current research.

Assuming a stable flexural wave advancing at a velocity of 10m/s, the temporal dependence at a given distance of both the Brillouin results (blue), as well as the input strain, as would be measured by a *short* FBG (green), appear in Fig. 6(b). The two techniques would produce similar results if temporal smoothing were applied to the FBG data (red curve in Fig. 6(b)). All these observations have been experimentally confirmed, see below.

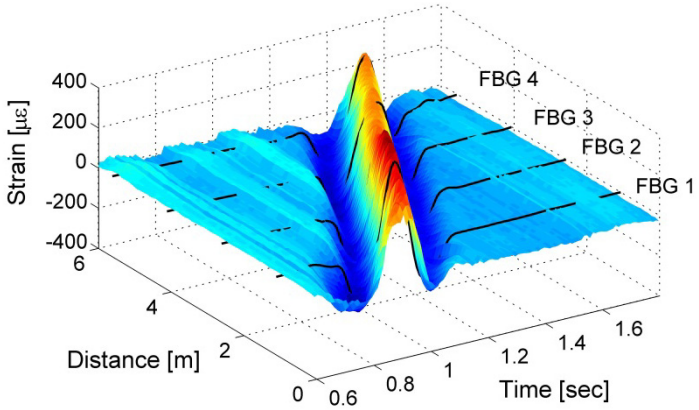

Fig. 7. The Brillouin measured SA-BOTDA *spatially and temporally continuous* results as a function of both time and distance for the first 6 meters of the strip. Results are compared with the data from the four spatially *discrete* FBGs (black lines). In Figs. 7-10 time is measured from an arbitrary origin, where data collection commenced (not to be confused with the time origin of the simulation of Fig. 6, which coincided with the moment the pump pulse entered the strip).

5. Measurements

Figure 7 shows the measured SA-BOTDA *spatially and temporally continuous* results as a function of both time and distance for the first 6 meters of the strip. We clearly see how the positive strains at the top of the wave turn negative at the leading and trailing edges. Also shown (black lines) are the temporal dependences of the strain, as measured at only four discrete locations by the FBGs. The column of four panels in Fig. 8(a) provides a closer comparison between the temporally aligned Brillouin and FBG results. Three curves are shown at each location: The Brillouin result (blue), the FBG results (low-pass filtered to 100Hz to remove noise; green), as well as smoothed versions of the FBG data over a time window of 50ms (red), mimicking spatially integrating 50cm long FBGs (assuming a wave velocity of 10m/s). Very nice agreement is achieved between the Brillouin and the smoothed FBG measurements. As predicted in Fig. 6, the unsmoothed 1cm FBGs (green) offer better resolution than that of the Brillouin data at a pump pulse width of 13ns. However, the FBGs

#184596 - $15.00 USD Received 31 Jan 2013; revised 13 Mar 2013; accepted 17 Mar 2013; published 24 Apr 2013

provide strain data only at their discrete locations, while the SA-BOTDA simultaneously produce a 2-D time and distance map of the dynamic strain, see Fig. 8(b).

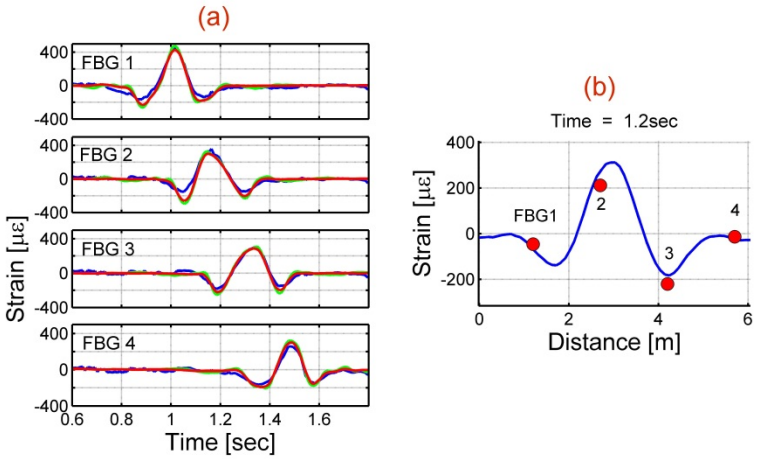

Fig. 8. (a) The time dependence of the strains at the locations of the four FBGs, as measured by: The SA-BOTDA (blue); 1cm spatial resolution FBGs (low-pass filtered to 100Hz and temporally aligned with the Brillouin data, green); A smoothed version of the FBG data (red). (b) A snapshot of the spatial distribution of the strain at t = 1.2sec, showing the continuous Brillouin results (blue) *vs.* the discrete nature of the FBG technique (red dots), Media 2.

Two different 3D views of the Brillouin-obtained strain which accompanies the propagation of a flexural wave from the strip beginning ($z = 0$) to the strip end ($z = 20\text{m}$) appear in Fig. 9. A few characteristics of the wave can be immediately deduced from the figures: (*i*) The wave weakens with distance; (*ii*) Its average velocity is ~9m/s; (*iii*) It speeds up towards the strip end. A lot more quantitative information can be inferred from a detailed study of various cuts through either the time or distance coordinates.

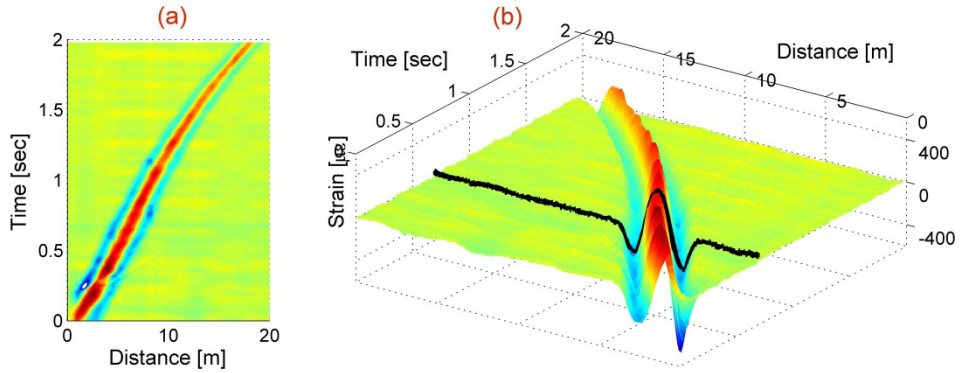

Fig. 9. Two 3D views of the strain accompanying the flexural wave as the latter propagates along the 20m tape with a velocity of ~9m/s. These figures clearly show that the wave slightly accelerates towards the end of the strip, while simultaneously decaying. The black curve in (b) represents a snapshot of the strain at t = 0.7s (Media 3).

In a second experiment, two mechanical waves were simultaneously launched at the two opposite ends of the strip (Fig. 10(a), taken from Media 4), giving rise to two counter-propagating waves. Figure 10(b), and also Media 5 quantitatively describes their courses of propagation, including the details of their collision.

#184596 - $15.00 USD Received 31 Jan 2013; revised 13 Mar 2013; accepted 17 Mar 2013; published 24 Apr 2013

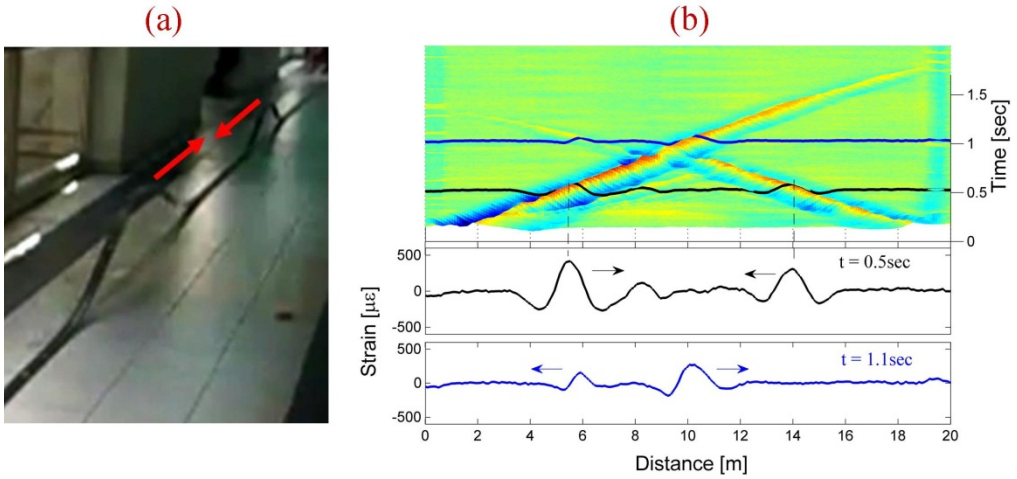

Fig. 10. Two counter-propagating flexural waves, simultaneously launched from the two ends of the strip. (a) A single frame from a movie (Media 4). (b) 3D and 2D snapshots from the measurement movie (Media 5) of the strain fields of the two counter-propagating flexural waves. The black and blue lines are 2D presentations of the strain distribution along the strip before (at t = 0.5 sec) and after (at t = 1.1 sec) their collision.

6. Discussion and summary

We have demonstrated a practical utilization of the SA-BOTDA method for monitoring mechanical waves, propagating along a composite stip. A standard SMF-28 optical fiber was attached to the strip surface, enabling distributed and dynamic measurement of the strain along its length, at a sampling rate (for the whole strip) of 100 samples/sec and spatial resolution of ~1m. For more demanding measurements, where the measured dynamic strain changes much faster, the same system and setup can provide much higher sampling rates limited only by the time of flight through the fiber and signal to noise ratio considerations. Spatial resolution can be also improved, either by using shorter pump pulses or by employing one of the available methods for spatial resolution enhancement [8–11].

In summary, this reported demonstration opens the way to many applications albeit with an obvious trade-off between spatial resolution, sampling rate and available signal-to-noise ratio.

Acknowledgments

This research was supported by the Israel Science Foundation (grant No. 1380/12).

#184596 - $15.00 USD Received 31 Jan 2013; revised 13 Mar 2013; accepted 17 Mar 2013; published 24 Apr 2013